# Metabolomics of heat stress response in pig adipose tissue reveals alteration of phospholipid and fatty acid composition during heat stress[1]

**Huan Qu and Kolapo M. Ajuwon[2]**

Department of Animal Sciences, Purdue University, West Lafayette, IN 47907-2054

**ABSTRACT:** To determine the effect of heat stress (**HS**) on adipose tissue metabolome, a combination of liquid chromatography-mass spectrometry–based metabolomics profiling approaches was applied to characterize changes of metabolite classes in adipocytes differentiated in culture (in vitro) and mesenteric adipose tissue of pigs exposed to HS (in vivo). Effect of HS on the composition of individual fatty acids in cultured adipocytes, mesenteric adipose tissue, and serum of animals was also investigated using gas chromatography analysis. In vitro, preadipocytes were differentiated either under control (37 °C) or HS (41.5 °C) temperature for 9 d. For the animal experiment, pigs were kept either in control (**Con**) environment (20 °C) with ad libitum feed intake, HS (35 °C) temperature with ad libitum feed intake (HS), or at 20 °C with pair feeding to the HS pigs. In cultured cells, HS increased triglyceride and decreased monoacylglycerol ($P < 0.05$) species accumulation compared with control. Phosphatidylinositol and phosphatidylserine were increased by HS, whereas phosphatidylcholine, phosphatidylethanolamine, and phosphatidylglycerol were decreased relative to control ($P < 0.05$). Heat-stressed adipocytes in culture also had higher concentrations of saturated (**SFA**) and monounsaturated fatty acids ($P < 0.05$) relative to control. Pathways of proline and biotin metabolism were elevated ($P < 0.05$) by HS in adipocytes. The metabolomics signatures in adipocytes cultured under HS indicates that pathways centered around diacylglycerol metabolism are impacted by HS. In adipose tissue from animals in the HS treatment, there was increased ($P < 0.05$) abundance of 4,8 dimethylnonanoyl carnitine ($P < 0.05$). Heat-stressed animals also had higher ($P < 005$) serum linoleic, total polyunsaturated fatty acids, and decreased total SFA than PF ($P < 0.05$). These results indicate that HS elevates lipogenic pathways while suppressing fatty acid oxidation and demonstrate the usefulness of metabolomics analysis as a tool for determining the impact of HS in pig tissues.

**Key words:** adipocyte; heat stress; lipidomics; lipids; metabolomics



J. Anim. Sci. 2018.96:3184–3195
doi: 10.1093/jas/sky127

## INTRODUCTION

Heat stress (**HS**) is a major environmental factor against optimal production efficiency in swine. An important adaptive response to HS is the induction of heat shock proteins (**HSP**) which help in heat adaptation (Feder and Hofmann, 1999). However, HS response also involves other mechanisms, such as alteration in lipid metabolism (Schmidt and Widdowson, 1967; Katsumata et al., 1990). This is because lipids play a very important role in regulation of several biological processes–involved HS response. Therefore, determining the impact of HS on lipid metabolites is an important step toward a better understanding of the role of different lipids in HS adaptation.

[1]This study was supported by a grant from the College of Agriculture, Purdue University, through the AgSEED funding mechanism.

[2]Corresponding author: kajuwon@purdue.edu

Received December 5, 2017.
Accepted April 4, 2018.

It has been demonstrated that HS increases lipid retention by decreasing lipolytic rates or increasing adipose tissue lipoprotein lipase in rodents (Schmidt and Widdowson, 1967; Katsumata et al., 1990), pigs (Heath, 1983; Christon, 1988), and chickens (Geraert et al., 1996). Additionally, in our earlier work (Qu et al., 2015), it was shown that HS could stimulate cell autonomous increase in lipogenesis and triglyceride storage in pig adipocytes (Qu et al., 2015). Therefore, changes in cellular and tissue lipid composition could indicate that alteration in lipid metabolism is an integral part of physiological and metabolic adaption to HS. In support of this possibility, it has been suggested that membrane lipid physical state could play an important role in the control of heat sensing and signaling (Escribá et al., 2008).

In Qu et al. (2016), we showed that HS resulted in increased expression of heat shock protein 70 (**HSP70**), CCAT/enhancer-binding homologous protein (**CHOP**) in the mesenteric fat compared with animals kept in thermoneutral environment. In addition, HS led to increased expression of phosphoenol pyruvate carboxykinase (**PCK1**), suggesting that HS might lead to tissue stress and elevated glyceroneogenesis in adipose tissue. There was also a modest increase in blood urea nitrogen (**BUN**) in male pigs in HS compared with control animals (Qu et al., 2016). However, these indicators did not provide a comprehensive insight into tissue responses to HS that could increase understanding of effect of HS in pigs. Metabolites and lipid species altered in HS may serve as useful biomarkers associated with HS response. Determining the identities of these metabolites may open a window for investigating the mechanism of HS sensing, signaling, and adaptation, and may provide information that can be utilized for achieving efficient animal production. Therefore, the objective of this experiment was to determine, using metabolomics analysis, a comprehensive impact of HS on lipid and nonlipid metabolites in adipocytes that were differentiated in vitro and mesenteric adipose tissue of pigs.

## MATERIALS AND METHODS

### *Experiment 1: Effects of HS in Pigs*

Purdue Animal Care and Use Committee (**PACUC**) approved all animal protocols described in this publication. Details of animal experimentation, tissue collection, and handling have been described in Qu et al. (2016). Ossabaw pigs (female $n = 15$, male $n = 15$) at 6 mo of age were randomly allocated to three treatments (female $n = 5$ and male $n = 5$ per treatment): control (**Con**) group with room temperature at 20 °C ± 1 °C and relative humidity 53% to 78%, and had ad libitum feed intake; pair-fed (**PF**) treatment with same room temperature and relative humidity as Con group, and PF to the feed intake of HS pigs; HS group with room temperature set at constant 35 °C ± 1 °C and relative humidity 45% to 65% with ad libitum feed intake. Pigs were penned individually and were allowed to adjust to their environment for 7 d before treatments were applied for another 7 d. Pigs in the pair-feeding treatment were fed twice daily at 0900 and 0500 h with a quantity of feed equal to the previous day's FI of pigs in the HS treatment. The feed met or exceeded the nutrient requirements of pigs of that age (NRC, 2012) (Table 1).

On day 7 of experiment, pigs were euthanized following sedation with intramuscular injection of atropine, tiletamine–zolazepam and xylazine, and asphyxiated with $CO_2$, followed by pneumothorax and cardiectomy while under anesthesia. Mesenteric adipose tissues were collected from areas flanking the mid-jejunum and flash frozen in liquid nitrogen before stored in −80 °C freezer. Blood was collected

**Table 1.** Feed ingredient composition (as-fed basis)

| Ingredient | Percentage |
|---|---|
| Corn | 79.75 |
| Soybean meal | 1.95 |
| Dried distiller's grains | 15.00 |
| Swine white grease | 1.00 |
| L-lysine | 0.38 |
| L-threonine[1] | 0.09 |
| L-tryptophan | 0.04 |
| Limestone | 1.14 |
| Monocal phosphate | 0.14 |
| Vitamin premix[2] | 0.10 |
| Sodium chloride | 0.25 |
| Selenium 270 premix[3] | 0.03 |
| Phytase[4] | 0.08 |
| Non-sulfur T.M. premix[5] | 0.05 |

[1]98% L-threonine.

[2]Swine vitamin premix: vitamin A, 544,680 IU/kg; vitamin D3, 54,448 IU/kg; vitamin E, 3631 IU/kg; menadione (vitamin K), 182 mg/kg; vitamin B12, 3.2 mg/kg; riboflavin, 726 mg/kg; d-pantothenic acid, 1,816 mg/kg; niacin, 2,723 mg/kg, biotin, 18.1 mg/kg; folic acid, 136 mg/kg; choline, 45,390 mg/kg; pyridoxine, 409 mg/kg; vitamin E, 1,816 IU/kg; chromium, 16.3 mg/kg; carnitine, 4,805 mg/kg.

[3]Selenium 270 premix: 600 mg/kg of selenium as sodium selenite in a mixture of equal portions of ground limestone and ground corn to fill 0.05% of the diet.

[4]600 ppm phytase.

[5]Non-sulfur trace mineral premix: iron, 51.05%; zinc, 20.73%; manganese, 2.86%; copper, 1.56%; iodine, 0.046%.

into Vacutainer tubes by jugular venipuncture before feeding on day 7 of the experiment. Serum was recovered from whole blood following centrifugation at 10,000 × *g* for 10 min at 4 °C.

### *Experiment 2: Cell Isolation and In Vitro Culture*

Isolation and culture of primary porcine preadipocytes were based on the protocol described previously (Ramsay, 2005; Qu et al., 2015). Briefly, preadipocytes (**SVC**) were isolated from the inner layer of subcutaneous adipose tissue from male juvenile piglets (<7 d old). Tissue was kept in buffered saline (0.15 M NaCl, 10 mM HEPES, pH 7.4) at 37 °C and cut into small pieces with a pair of sterile scissors followed by incubation in a digestion cocktail (10 mM $NaHCO_3$, 10 mM HEPES, 5 mM D-glucose, 120 mM NaCl, 4.6 mM KCl, 1.25 mM $CaCl_2$, 1.20 mM $MgSO_4$, 1.20 mM $KH_2PO_4$, 3% BSA) containing collagenase (collagenase type I, 1mg/mL, Worthington Biochemical Corp., Lakewood, NJ) in a shaking water bath at 37 °C for 45 min at 120 oscillation/min. Adipocytes were separated from SVC pellet by centrifugation at 2,000 × *g* for 10 min at 4 °C. The SVC was washed twice in the digestion cocktail. The SVC pellet was resuspended in Dulbecco's modified Eagle's medium/F12 (**DMEM/F12**) medium (Sigma-Aldrich, St. Louis, MO) with 10% fetal bovine serum (**FBS**; Mediatech, Manassas, VA), 1% antibiotic-antimycotic (Sigma-Aldrich) and incubated in a humidified incubator with 5% $CO_2$ and 95% air. Cells were differentiated under normal (37 °C) or HS (41.5 °C) temperature environments for 9 d in a differentiation medium: DMEM/F12 with 10% FBS, 1% antibiotic-antimycotic, 1 µM insulin, 1 µM dexamethasone (1 mM), 1µM rosiglitazone, 1 µM biotin, 1 µM triiodothyronine (**T3**), 1 µM pantothenic acid after reaching confluence. Medium was replaced every 3 d and rosiglitazone was removed from the differentiation media after day 3 of differentiation. Cells were fully lipid-filled by day 9.

### *Sample Preparation for Metabolomics Analysis*

Adipocytes from the in vitro experiment cultured at either 37 °C or 41.5 °C conditions as described above were scraped into microcentrifuge tubes and homogenized in 4 mL/g of cold methanol and 0.85 mL/g cold water. Only mesenteric adipose tissues from HS and PF pigs were compared. Frozen mesenteric adipose tissues were thawed on ice and homogenized in cold methanol as described for adipocytes. Both adipocyte and mesenteric adipose tissue samples were processed similarly thereafter. Cold chloroform (4 mL/g) and 2 mL/g cold water were added. Samples were then vortexed for 60 s and kept on ice for 10 min to allow phase separation and thereafter centrifuged for 10 min at 10,000 × *g* at 4 °C to remove precipitated proteins and tissue debris. The upper polar phase was transferred into new Eppendorf tube for metabolomics analysis of polar compounds and the lower nonpolar organic (lipids) phase into a new tube for metabolomics (lipidomics) analyses (Wu et al., 2008).

### *Nontargeted Metabolomics Analysis of Polar and Nonpolar (Lipids) Compounds*

The analysis was performed on an Agilent 1100 series HPLC system coupled to an Agilent MSD-TOF (time-of-flight) MS (Agilent Technologies, Santa Clara, CA). The compounds were separated using a Waters Atlantis T3 column (150 mm × 2.1 mm, 3-µm particle size) in a 50-min run at 30 °C with an injection volume of 5 µL. A gradient extraction procedure was applied using a binary mobile phase composed of 0.1% formic acid (v/v) in double-distilled water (eluent A) and 0.1% formic acid (v/v) in acetonitrile (eluent B) at a flow rate of 0.3 mL/min. The following linear gradient program was applied: 0 min, 0% B; 1 min, 0% B; 39 min, 80% B; 40 min, 0% B; 50 min, 0% B. The MS was equipped with an electrospray ionization (**ES**) source. The data generated were collected with a mass-to-charge ratio (m/z) in the range of 75 to 1,000 with a 1.4 spectra/s acquisition rate. The operating conditions for ESI were as follows: nebulizer gas (N2) pressure, 35 psi; drying gas (N2) flow, 9.0 L/min; and drying gas temperature, 350 °C. The capillary and fragmentor voltages were set at 3,500 and 135 V, respectively. Accurate mass calibration was carried out by the continuous infusion of Agilent Reference Mass Solution (reference number G1969-85001) using the following reference masses: 121.0509 and 922.0098 m/z.

Nontargeted metabolomics analysis of nonpolar organic compounds (lipids) was performed on the same Agilent 1100 system using a Waters Xterra MS C18 column (5 µm, 150 × 2.1 mm i.d.) with an injection volume of 10 µL. A binary mobile phase consisting of solvent systems A and B were used in gradient elution where A was water, 10 mM ammonium acetate, 0.1% formic acid (v/v), and B was 50% acetonitrile, 50% isopropyl alcohol, 10 mM ammonium acetate, 0.1% formic acid (v/v). The mobile phase flow rate was 0.3 mL/min. Initial conditions were set at 65:35 A: B and held for 1 min,

followed by a linear gradient to 20:80 from 1 to 10 min, followed by a linear gradient to 0:100 from 10 to 20 min and held at 0:100 for 12 min. Gradient conditions were re-equilibrated to 65:35 A: B from 32 to 33 min and held for 7 min at initial conditions prior to the next run. Following separation, the column effluent was introduced by positive or negative mode ESI into an Agilent MSD-TOF spectrometer. ESI capillary voltage was 3.5 kV, nebulizer gas pressure was set at 35 psi, gas temperature was 350 °C, drying gas flow rate was 9.0 L/min, fragmentor voltage was set to 135 V, skimmer 60 V and OCT RF V 250 V. Mass data (m/z 100–1,200) were acquired and analyzed using Agilent Mass Hunter software. The mass data led to identification of precursor ion masses and specific compounds with relative abundance given by the ratio or fold of their peak area in the chromatogram generated compared to the control. Accurate mass determination was ensured by the continuous infusion of Agilent Reference Mass Solution (G1969-85001).

### *Gas Chromatography Analysis of Fatty Acid Methyl Esters*

Total lipids from in vitro differentiated adipocytes, serum, and mesenteric adipose tissue were extracted based on the modified method of (Folch et al., 1957). Samples were extracted in a 2:1 (vol/vol) chloroform: methanol organic solvent mixture. Fatty acid methyl esters (**FAME**) were prepared and dissolved in hexane for gas chromatography (**GC**) analysis. The FAME were quantified using an Agilent 7890 GC equipped with an FID detector and also Agilent 5975 MSD detector (Agilent). The GC/FID was equipped with a 60 m DB-5 capillary column (0.25 mm ID, 0.25 µm film thickness; J&W Scientific). The FAME were identified by retention time and fragmentation pattern and quantified by peak area against a standard (Supelco 37 component FAME mix; Sigma-Aldrich). The GC/MSD analysis used a rt-2560 capillary column (100 m × 0.25 mm with internal diameter; 0.2 µm film thickness; Restek, Bellefonte, PA). The GC/FID detector temperature program was set to 90 °C to 180 °C at 10 °C/min, then to 285 °C at 3 °C/min; injector temperature 200 °C, detector temperature 290 °C. Total run time 47 min. GC/MSD detector temperature program was set to 50 °C for 5 min to 125 °C at 10 °C/min, then to 250 °C at 4 °C/min hold 12.25 min; injector temperature 250 °C, detector temperature 300 °C. Total run time 56 min. Results were presented and analyzed as a molar percentage of total FAME.

### *Data Processing and Statistical Analysis*

Agilent's Mass Hunter Qualitative Analysis software (v. B.06) was used to identify individual chromatographic peaks. The Molecular Feature Extraction algorithm was used as a first pass, followed by the Find by Ion algorithm. Agilent's Mass Profiler Professional software (v. 12.6.1) was used to identify statistically significant biomarkers. Peaks were aligned across all samples in a data set to account for instrumental drifts in retention time and mass. Each compound was normalized first by external scalar (to account for sample weights), and then Percentile Shift (using 75% option). Compounds were baselined, then Filtered on Flags, retaining only compounds that appeared in two or more samples. Compounds were then Filtered by Frequency, keeping only compounds that appeared in a defined percentage of samples in at least one treatment type. A principal component analysis (**PCA**) plot was generated with a quality control step to identify possible outliers. A *t* test was performed to compare treatment differences. A fold change criteria were employed whereby samples from HS treatments were compared to control and these ratios statistically analyzed. Statistically significant compounds determined by *t* test analysis between control and HS treatments were queried on the Human Metabolome Database (**HMDB**) and the MetaCore software (Encinitas, CA) was used for pathway analysis. A peak must be present in four out of six samples to determine presence/absence. Comparisons to assess the significance of differences in fatty acid profiles in adipocyte were performed using one-way ANOVA with a Tukey HSD post hoc test. Differences in tissues and sera were analyzed with two-way ANOVA followed with the Tukey comparison test.

## RESULTS

### *Animal Performance in Response to HS*

Performance responses of animals in response to treatment have been previously described in detail (Qu et al., 2016). Briefly, pigs in the HS treatment had approximately 40% lower FI in comparison to the CON treatment ($P < 0.01$). However, as designed, the FI of the PF pigs was similar to that of the HS pigs. There were no differences in final BW and daily gain in all treatments. The HS pigs had elevated skin temperature (+6 °C) and a 2-fold increase in respiration rate compared with CON

and PF pigs ($P < 0.01$). Final rectal temperature was +0.3 °C higher (38.6 vs. 38.9 °C, $P < 0.05$) in HS pigs than CON and PF. There was a tendency for a higher ($P < 0.06$) expression of HSP70 in the mesenteric adipose tissue of HS pigs compared to CON (2 fold) and PF (1.5 fold) pigs. There was also a significant increase ($P < 0.01$) in the expression of PCK1 in the mesenteric adipose tissue of HS pigs compared to CON (10.7 fold) and PF (4 fold). Plasma metabolites such as triacylglycerol (**TAG**), free fatty acids (**FFA**), and glucose were not affected by treatment. However, males in HS had elevated (1.4 fold, $P < 0.05$) BUN relative to males in the CON treatment.

### *Effects of HS on Adipocyte Lipidome (Nonpolar Compounds)*

A total of 3,494 ionic species were detected using both positive and negative ionizations in a nontargeted approach. Multivariate analyses were used to explore the differences between locations. Due to the similarities in the patterns of results from both negative and positive ionizations by PCA, only the positive ionization results are shown. As the PCA plots of nonpolar compounds show (Fig. 1), samples were separated based on temperature. The heat map shows that the abundance of several lipids was different between CON and HS treatments (Supplementary Fig. 1). The whole lipidome reveals that 718 lipid species were significantly different between control and heat-stressed adipocytes. The lipid species that were identified were further separated by their classes and expressed based on whether their total count was increased or decreased in HS relative to control. Among them were glycerophospholipids, glycerolipids, sphingolipids, steroids and steroid derivatives, prenol lipids, linoleic acids and derivatives, and fatty acyls (Fig. 2A). Among the glycerophospholipid species, glycerophosphoserines, glycerophosphoglycerols, glycerophosphoethanolamines, glycerophosphoinositols, glycerophosphoglycerophosphates, and glycerophosphates were identified (Fig. 2B). Phosphatidylcholine and phosphatidylethanolamine were the two most-affected glycerophospholipids.

Glycerolipids were classified to triglycerides, diacylglycerols (**DAG**), and monoacylglycerols (Fig. 2C). Triglycerides were the most abundant in the HS group, and monoacylglycerols were most abundant in the control group. A comprehensive list of lipid metabolites is presented in Supplementary Table 1.

### *Effects of HS on the Metabolome of Polar Compounds in Adipocytes*

The metabolome of polar compounds also separated by temperature using PCA (Fig. 3A). The heat map showed two distinct patterns of regulation of the compounds and indicates that the abundance of several compounds was inversely regulated in HS and control (Supplementary Fig. 2). Additionally, metabolomics pathway analysis (Fig. 3B) revealed upregulation of several metabolic pathways including proline, deoxyguanosine triphosphate (**dGTP**), biotin, insulin, galactose, acetyl-CoA, and transcription factor carbohydrate response element-binding protein metabolism by HS.

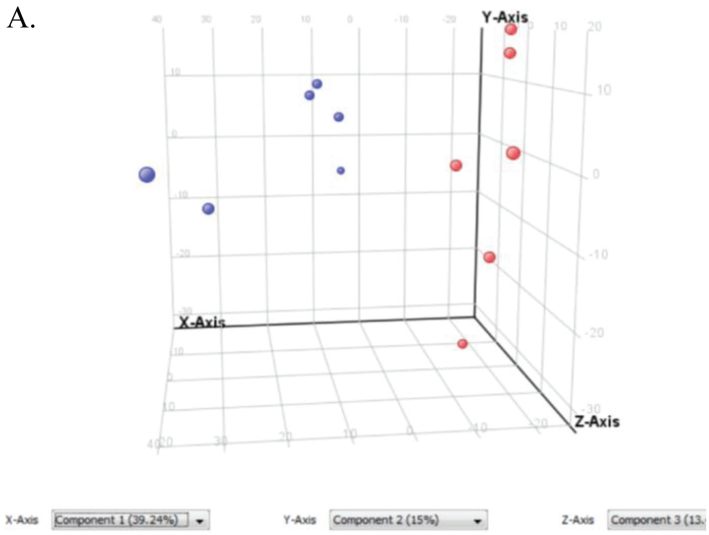


**Figure 1.** Principal component analysis (PCA) and heat map of metabolomics analysis of nonpolar compounds in in vitro differentiated adipocytes. PCA analysis, metabolites were separated by temperature using PCA.

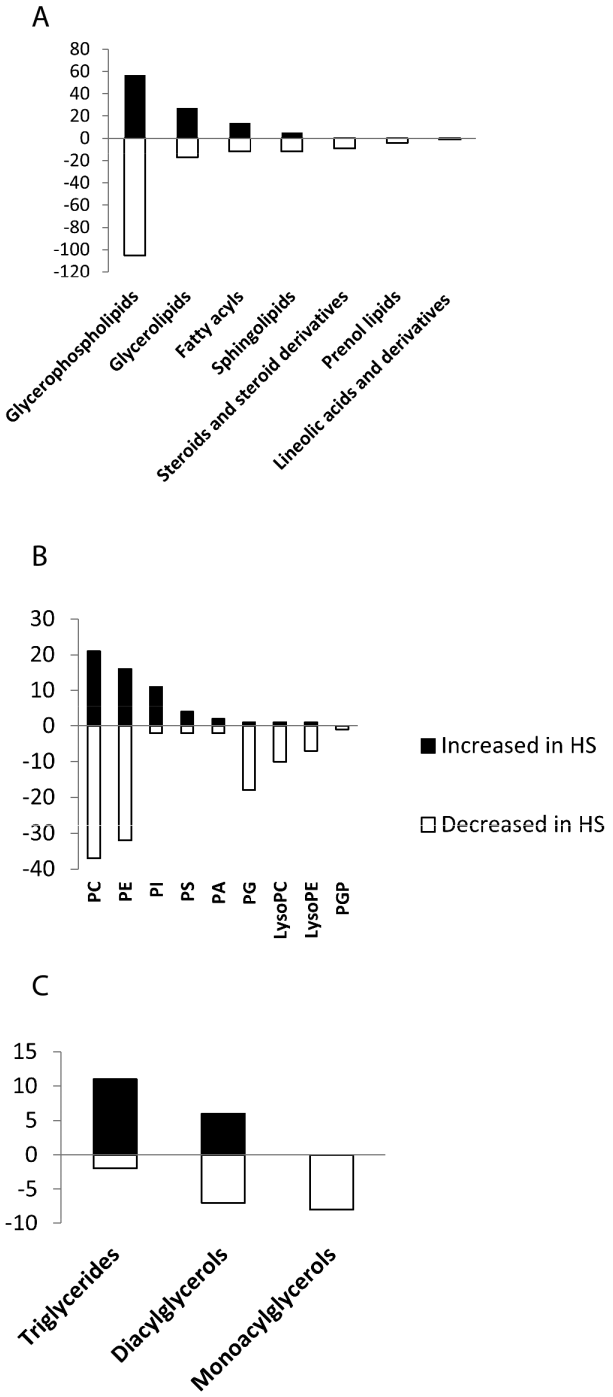


**Figure 2.** Abundance of different species of nonpolar metabolites showing numbers that are increased or decreased in adipocytes exposed to heat stress (41.5 °C) relative to the control (37 °C). (A) Number of the different molecular species according to their categories. (B) Number of different glycerolphospholipids. (C) Number of different glycerolipids. Bars represent number of species (black bars indicate number increased and open bars indicate number decreased in HS compared to control).

### *Effects of HS on Mesenteric Adipose Tissue Lipidome (Nonpolar Compounds)*

The PCA plot of mesenteric fat nonpolar compounds indicates gender effects in the separation of metabolites such that the metabolites separated better by temperature better in the boars (Fig. 4A) than gilts (Fig. 4B). There was also a higher ($P < 0.05$) amount of PE (18:0/22:1(13Z) and PC (16:1(9Z)/20:0) in boars in HS than PF (Fig. 4C).

### *Effects of HS on the Metabolome of Polar Compounds in the Mesenteric Adipose Tissue*

The PCA plot of polar compounds reveals a clear separation between the PF and HS treatments in the boars (Fig. 5A) and gilts (Fig. 5B). Metabolic pathway analysis revealed increased ($P < 0.05$) metabolism of arginine, adenine, 4,8 dimethylnonanoyl carnitine in gilts in HS than PF (Fig. 5C).

### *Fatty Acid Profiles of Adipocyte, Serum, and Mesenteric Adipose Tissue*

Adipocyte fatty acid profile is presented in Table 2. Adipocytes in HS had a greater proportion of total saturated fatty acids (**SFA**) than Con, and higher ($P < 0.05$) composition of myristic (C14:0) and palmitic (C16:0) acids than any other single fatty acid (9.57% and 30.52% increase, respectively). Adipocytes in HS also had a lower ($P < 0.05$) proportion (21.81% decrease) of monounsaturated fatty acids (**MUFA**) and lower MUFA:SFA ratio than Con. The composition of the MUFA palmitoleic (C16:1) was lower ($P < 0.001$) in the HS group than Con (57.30% decrease). Additionally, linoleic (C18:2n6c) and eicosapentaenoic acid (20:5n3), both polyunsaturated fatty acid (**PUFA**) were lower ($P < 0.05$) in HS treatment (39.43% and 15.00% decreases, respectively) than Con.

Serum fatty acid profile is presented in Table 3. Concentration of stearic acid (C18:0) was decreased in HS (17.32% decrease) compared to PF ($P < 0.002$). However, there was an increase in linoleic acid in the serum of HS pigs compared to PF (43.91% increase; $P < 0.004$). There was a decrease ($P < 0.003$) in total SFA in HS relative to PF (8.6% decrease). However, total PUFA increased (33.38%; $P < 005$) in HS pigs relative to PF. Therefore, the PUFA/SFA ratio was higher ($P < 0.003$) in HS than PF and control. Fatty acid analysis of mesenteric adipose tissue is presented in Table 4. There was no effect of treatment on the overall fatty acid profile, although gilts had a lower ($P < 0.002$) level of linoleic acid, higher ($P < 0.03$) level of gadoleic acid and a lower PUFA/SFA ratio ($P < 0.028$) than boars.

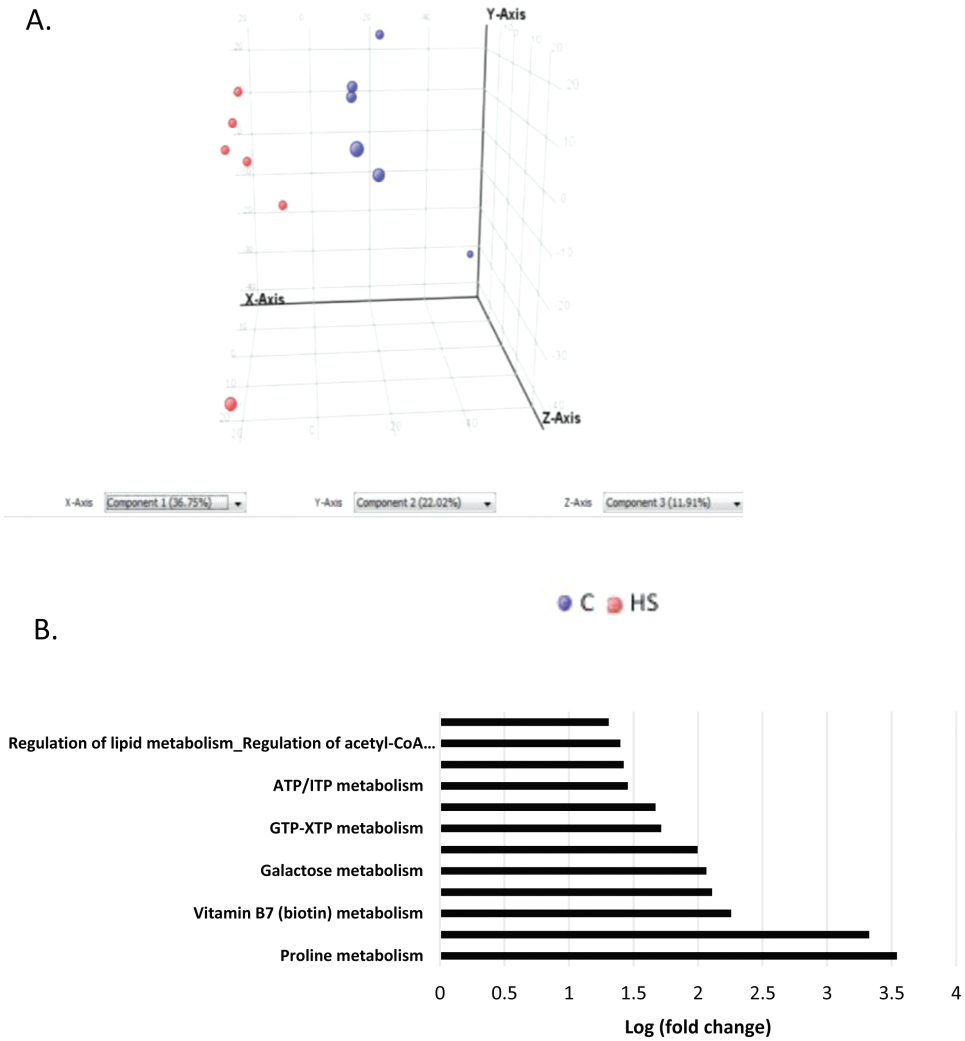


**Figure 3.** Principal component analysis (PCA), heat map and pathway analysis of metabolomics analysis of polar compounds in in vitro differentiated adipocytes. (A) PCA analysis, metabolites were separated by temperature using PCA. (B) Pathway analysis showing fold upregulation of specific metabolic pathways in HS compared to control.

## DISCUSSION

Previous studies have shown that HS causes increased lipid retention in rodents (Schmidt and Widdowson, 1967; Katsumata et al., 1990), pigs (Heath, 1983; Christon, 1988), and chickens (Geraert et al., 1996). Kellner et al. (2016) found a reduction in the expression of lipolytic genes in pigs subjected to HS and this led to increased carcass fat compared to PF thermoneutral controls. We have also demonstrated (Qu et al., 2015) that HS increased de novo lipogenesis and triglyceride storage in pig adipocyte. Thus, there was a need to get a better understanding of effects of HS on lipid metabolism and metabolite changes in pigs. In contrast, other studies showed that HS resulted in leaner carcasses in pigs (Cruzen et al., 2015; Johnson et al., 2015), and studies by Sanz-Fernandez et al. (2015) did not find any significant effect of HS on markers of insulin sensitivity in adipose tissue in pigs.

Differences in measures of adiposity or adipose-specific responses to HS from different investigators likely reflect effects of dissimilar experimental conditions such as duration and intensity of HS and whether heat-stressed pigs were being compared to ad libitum fed pigs kept in thermoneutral temperature or with those that were PF to heat-stressed pigs, as we have done in this study, to account for potential effects of feed intake differences. In any case, determining comprehensive changes in lipid and other metabolite classes are needed to elucidate mechanism of HS response in pigs. Such an understanding could be useful for developing better management strategies for dealing with the negative consequences of HS in pigs.

Adipose pig adipocytes grown in culture respond to HS with increased triglyceride storage (Qu et al., 2015). Our previous work in pigs exposed to HS has also shown that HS in pigs is accompanied by adipose tissue–specific responses that favor

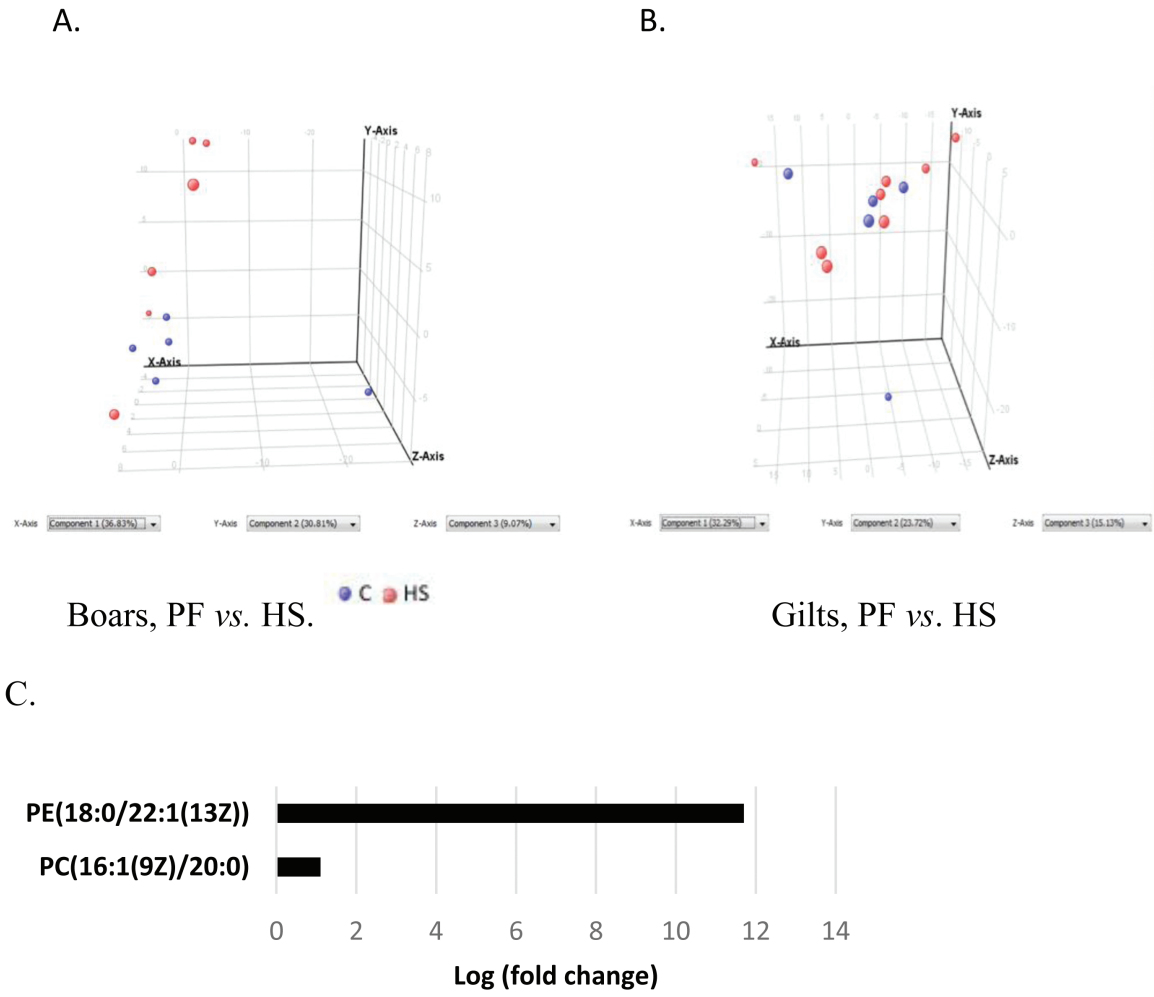


**Figure 4.** Principal component analysis (PCA) and metabolomics analysis of nonpolar compounds of pigs kept at normal room temperature (20 °C) and pair-fed (PF) to the feed intake of animals in heat stress (HS) (35 °C) for 1 wk. (A). Differences between boars in PF or HS treatments. (B) Differences between gilts in PF or HS treatments (C) Pathway analysis of nonpolar metabolites in boars in PF or HS treatments showing pathways that are upregulated in HS relative to PF.

increased triglyceride storage due to increased expression of PCK1, a lipogenic enzyme (Qu et al., 2016). This observation is confirmed in the metabolomics analysis and breakdown of glycerolipids conducted in this study, especially from the in vitro differentiated adipocytes. The reduction in monoacylglycerols and DAG and the upregulated TAG species (Fig. 2C) in HS adipocytes support a greater accumulation of TAG in adipocytes during HS at the expense of monoacylglycerols and DAG. In parallel, we also found increased metabolism of biotin and acetyl-CoA metabolic pathways. Biotin is a cofactor that is used by the enzyme acetyl-CoA carboxylase for the synthesis of malonyl-CoA, in the first committed step of fatty acid synthesis (Chang et al., 1967). Thus, the metabolomics analysis suggests increased utilization of acetyl-CoA for fatty acid and TAG synthesis during HS. This may be due to reduction of oxidation of substrates such as glucose during HS in adipocytes exposed to HS in vitro.

The default fatty acid from activities of acetyl-CoA carboxylase and fatty acid synthase (**FAS**) is palmitic acid (Smith, 1994). In support of increased de novo fatty acid synthesis, concentration of palmitate abundance was increased in adipocytes in HS in vitro (Table 2). This result is consistent with our previous finding that HS leads to increased FAS expression in pig adipocytes grown in culture (Qu et al., 2015). In addition, HS leads to increased concentration of palmitoleic acid (C16:1) in heat-stressed adipocytes (Table 2). This raises the possibility of increased activity of steroyl-CoA desaturase (**SCD1**) for the desaturation of palmitic acid to palmitoleic acid (Enoch et al., 1976) during HS. Increased palmitic acid concentration in adipocytes under HS indicates a potential role of this fatty acid in the regulation of cellular membrane fluidity as part of the mechanism of homeoviscous adaptation to HS (Ernst et al., 2016). It is known that HS induces fluidization of cellular membranes (Vigh et al., 1998; Leach and Cowen, 2014).

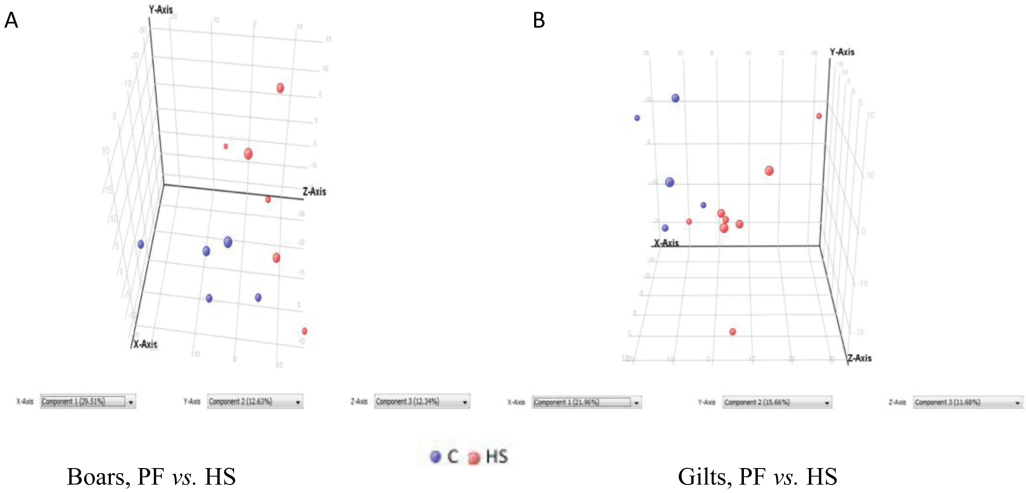


C.

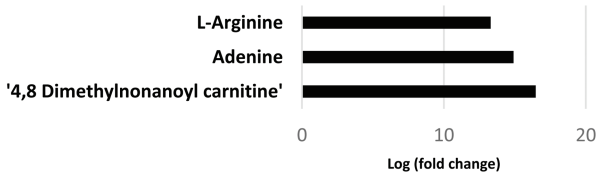


Metabolomics analysis Gilt (HS/PF)

**Figure 5.** Principal component analysis (PCA) and metabolomics analysis of polar compounds of pigs kept at normal room temperature (20 °C) and pair-fed (PF) to the feed intake of animals in heat stress (HS) (35 °C) for 1 wk. (A). Differences between boars in PF or HS treatments. (B) Differences between gilts in PF or HS treatments (C) Pathway analysis of nonpolar metabolites in gilts in PF or HS treatments showing pathways that are upregulated in HS relative to PF.

**Table 2.** Fatty acid profile of adipocytes

| Fatty acid (%)[1] | Control | Heat stress | SEM | *P* value |
|---|---|---|---|---|
| C12:0 (lauric acid) | 0.23 | 0.33 | 0.03 | 0.415 |
| C14:0 (myristic acid) | 1.88 | 2.06 | 0.04 | 0.004 |
| C16:0 (palmitic acid) | 29.82 | 38.92 | 0.91 | <0.001 |
| C16:1 (palmitoleic acid) | 17.05 | 7.28 | 1.76 | <0.001 |
| C18:0 (stearic acid) | 16.23 | 18.42 | 1.42 | 0.991 |
| C18:1n9c (oleic acid) | 25.94 | 20.27 | 1.11 | 0.885 |
| C18:2n6c (linoleic acid) | 3.17 | 1.92 | 0.41 | 0.030 |
| C18:3n6c (γ-linolenic acid) | 0.02 | 0.01 | 0.003 | 0.126 |
| C20:1n9 cis-11-eicosenoic acid (gadoleic acid) | 1.81 | 7.48 | 0.67 | <0.001 |
| C22:0 (behenic acid) | 0.27 | 0.22 | 0.03 | 0.121 |
| C20:5n3 (eicosapentaenoic acid, EPA) | 0.40 | 0.34 | 0.02 | 0.010 |
| C24:0 (lignoceric acid) | 0.53 | 0.38 | 0.05 | 0.006 |
| C22:6n3 (docosahexaenoic acid, DHA) | 2.66 | 2.81 | 0.06 | 0.402 |
| Total SFA | 48.96 | 60.33 | 1.58 | <0.001 |
| Total MUFA | 44.80 | 35.03 | 1.48 | <0.001 |
| Total PUFA | 6.25 | 5.08 | 0.52 | 0.421 |
| MUFA/SFA | 0.92 | 0.58 | 0.03 | <0.001 |
| PUFA/SFA | 0.13 | 0.08 | 0.01 | 0.077 |

MUFA = monounsaturated fatty acid; PUFA = polyunsaturated fatty acid; SFA = saturated fatty acid.

[1]Individual fatty acids are expressed as percentages of the total.

**Table 3.** Fatty acid profile of serum

| | Treatment | | Gender | | | | | *P* value | |
|---|---|---|---|---|---|---|---|---|---|
| Fatty acid (%)[1] | Con | PF | HS | Boar | Gilt | SEM | Trt | Gender | Interaction |
| C12:0 (lauric acid) | 0.44 | 0.60 | 0.87 | 0.98 | 0.45 | 0.10 | 0.217 | 0.007 | 0.933 |
| C14:0 (myristic acid) | 0.58 | 0.76 | 0.49 | 0.55 | 0.59 | 0.04 | 0.110 | 0.972 | 0.655 |
| C16:0 (palmitic acid) | 25.65 | 25.77 | 25.46 | 25.84 | 25.40 | 0.31 | 0.836 | 0.771 | 0.031 |
| C16:1 (palmitoleic acid) | 0.65 | 0.72 | 0.57 | 0.40 | 0.80 | 0.10 | 0.991 | 0.030 | 0.947 |
| C18:0 (stearic acid) | 29.23[a] | 30.32[a] | 25.07[b] | 28.34 | 26.92 | 0.69 | 0.002 | 0.236 | 0.204 |
| C18:1n9t (elaidic acid) | 0.62 | 0.48 | 0.23 | 0.14 | 0.61 | 0.09 | 0.179 | 0.014 | 0.111 |
| C18:1n9c (oleic acid) | 25.03 | 26.80 | 26.55 | 25.03 | 26.94 | 0.40 | 0.153 | 0.014 | 0.682 |
| C18:2n6c (linoleic acid) | 17.74[ab] | 14.37[b] | 20.68[a] | 18.63 | 18.20 | 0.78 | 0.004 | 0.522 | 0.212 |
| C18:3n6c (γ-linolenic acid) | 0.03 | 0.04 | 0.04 | 0.04 | 0.04 | 0.006 | 0.969 | 0.654 | 0.080 |
| C20:3n6 (dihomo-γ-linolenic acid) | 0.03 | 0.14 | 0.03 | 0.07 | 0.04 | 0.02 | 0.320 | 0.156 | 0.179 |
| Total SFA | 57.24[a] | 56.28[a] | 51.4[b] | 54.65 | 53.66 | 0.86 | 0.003 | 0.131 | 0.008 |
| Total MUFA | 25.55 | 27.82 | 27.37 | 25.80 | 27.57 | 0.43 | 0.288 | 0.001 | 0.133 |
| Total PUFA | 17.21[b] | 15.91[b] | 21.22[a] | 19.55 | 18.78 | 0.77 | 0.005 | 0.398 | 0.001 |
| MUFA/SFA | 0.45 | 0.50 | 0.54 | 0.47 | 0.52 | 0.01 | 0.059 | 0.002 | 0.079 |
| PUFA/SFA | 0.30[b] | 0.29[b] | 0.42[a] | 0.36 | 0.36 | 0.02 | 0.003 | 0.896 | 0.001 |

MUFA = monounsaturated fatty acid; PUFA = polyunsaturated fatty acid; SFA = saturated fatty acid.

[1]Individual fatty acids are expressed as percentages of the total.

[a,b]Significant mean differences between Con, PF, and HS treatments, $P < 0.05$.

**Table 4.** Fatty acid profile of mesenteric adipose tissue

| | Treatment | | Gender | | | | | *P* value | |
|---|---|---|---|---|---|---|---|---|---|
| Fatty acid (%)[1] | Con | PF | HS | Boar | Gilt | SEM | Trt | Gender | Interaction |
| C12:0 (lauric acid) | 0.09 | 0.10 | 0.09 | 0.10 | 0.09 | 0.01 | 0.922 | 0.548 | 0.211 |
| C14:0 (myristic acid) | 1.70 | 1.56 | 1.49 | 1.53 | 1.63 | 0.07 | 0.421 | 0.299 | 0.231 |
| C16:0 (palmitic acid) | 28.27 | 28.92 | 28.24 | 27.50 | 29.44 | 0.64 | 0.880 | 0.461 | 0.176 |
| C16:1 (palmitoleic acid) | 2.22 | 1.88 | 1.68 | 1.96 | 1.90 | 0.13 | 0.133 | 0.493 | 0.231 |
| C18:0 (stearic acid) | 12.47 | 12.15 | 11.88 | 12.12 | 12.28 | 0.63 | 0.848 | 0.367 | 0.667 |
| C18:1n9t (elaidic acid) | 0.24 | 0.27 | 0.24 | 0.25 | 0.25 | 0.02 | 0.862 | 0.735 | 0.654 |
| C18:1n9c (oleic acid) | 41.78 | 41.41 | 41.06 | 40.77 | 41.65 | 0.91 | 0.171 | 0.888 | 0.025 |
| C18:2n6c (linoleic acid) | 11.78 | 11.97 | 13.65 | 14.11 | 11.02 | 0.64 | 0.318 | 0.002 | 0.320 |
| C18:3n3,9,12 α-linolenic (alpha linolenic acid) | 0.43 | 0.54 | 0.59 | 0.50 | 0.56 | 0.02 | 0.194 | 0.875 | 0.671 |
| C20:1n9 cis-11-eicosenoic acid (gadoleic acid) | 0.79 | 0.81 | 0.74 | 0.71 | 0.87 | 0.04 | 0.720 | 0.031 | 0.972 |
| C20:3n6 (dihomo-γ-linolenic acid) | 0.13 | 0.27 | 0.23 | 0.24 | 0.19 | 0.04 | 0.352 | 0.856 | 0.107 |
| C20:4n6 (arachidonic acid) | 0.09 | 0.10 | 0.11 | 0.09 | 0.10 | 0.01 | 0.532 | 0.630 | 0.762 |
| Total SFA | 42.53 | 42.73 | 41.7 | 41.25 | 43.44 | 1.22 | 0.912 | 0.414 | 0.293 |
| Total MUFA | 45.03 | 44.37 | 43.72 | 43.69 | 44.67 | 1.72 | 0.884 | 0.529 | 0.238 |
| Total PUFA | 12.43 | 12.88 | 14.58 | 14.94 | 11.87 | 0.92 | 0.297 | 0.097 | 0.543 |
| MUFA/SFA | 1.06 | 1.04 | 1.05 | 1.06 | 1.03 | 0.06 | 0.895 | 0.896 | 0.226 |
| PUFA/SFA | 0.29 | 0.30 | 0.35 | 0.36 | 0.27 | 0.02 | 0.104 | 0.028 | 0.846 |

MUFA = monounsaturated fatty acid; PUFA = polyunsaturated fatty acid; SFA = saturated fatty acid.

[1]Individual fatty acids are expressed as percentages of the total.

Because fluidity of the cell membrane is important for membrane function, cellular membrane fluidity is maintained within a narrow range through homeoviscous adaptation to maintain cellular function under HS (Dymond, 2015). Thus, increased synthesis of palmitate, a SFA, under HS may suggest its increased use to counter the increased membrane fluidity caused by HS. Indeed, the abundance of phosphatidylcholine species with two palmitic acids (PC (16:0/16:0)) was increased in heat-stressed in vitro differentiated adipocytes. The most abundant membrane phospholipid is phosphatidylcholine

(van Meer et al., 2008). Thus, increasing the abundance of this saturated phosphatidylcholine might be an adaptive mechanism to correct the fluidization of adipocyte membrane by HS. This is presumably through an increase in the concentration of phosphatidylcholine species with SFA which are expected to decrease membrane fluidity.

Pathway analysis of in vitro cultured adipocytes under HS also show enhanced proline metabolism pathway. Metabolism of proline to 4-hydroxyproline is essential for the thermal stability of the collagen triple helix. Collagen that lacks hydroxyproline residues has a lower stability and melting temperature (Kubow et al., 2015). Although HS increases triglyceride synthesis, it causes membrane fluidity. Thus, increased production of collagen with 4-hydroxyproline might be an attempt to increase cellular rigidity to counter the fluidization that is brought about by HS. Therefore, regulation of extracellular matrix structure might be part of the adaptive response to HS in the adipocyte. On the other hand, proline has a potential a role to suppress reactive oxygen species (**ROS**) and apoptosis in mammalian cells (Krishnan et al., 2008) and increased proline metabolic pathway might direct proline to this anti-ROS and anti-apoptotic functions as well.

In the animal experiment, we chose a pair-feeding strategy to allow separation of observed effects that were due to differences in feed intake between animals in control environment vs. those in HS environment. Indeed, this need informed our choice of the PF and HS serum and mesenteric adipose tissue samples for the metabolomics analyses. Thus, responses obtained were independent of feed intake reduction. Mesenteric adipose tissue was chosen for the metabolomics analysis because we found this tissue to show the greatest changes in metabolic makers, relative to subcutaneous adipose tissue, as described in Qu et al. (2016). However, the metabolomics profile in the mesenteric adipose tissue of pigs under HS was not as clearly separated as in the in vitro differentiated adipocytes. However, increased accumulation of PE (18:0/22:1(13Z)) and PC (16:1(9Z)/20:0) might also help to increase tissue rigidity to counter the fluidization of mesenteric adipose tissue caused by HS. The increased accumulation of 4,8 dimethylnonanoyl carnitine, a fatty acid oxidation intermediate product may reflect impairment of fatty acid oxidation in adipose tissue in HS, hence accumulation of this intermediary product. At present, the potential biological implication of the elevated adenine and L-arginine metabolism is unknown, although increased L-arginine metabolism might indicate increased proteolysis of proteins in adipose tissue of pigs under HS. Increased L-arginine might also provide increased level of this precursor for nitric oxide synthesis (Stuehr, 2004), perhaps to increase tissue blood flow (Ardilouze et al., 2004) during HS.

The lower concentration of serum stearic acid and the lower total SFA in heat-stressed pigs may suggest an increased withdrawal of SFA into tissues, perhaps to be used for increasing tissue rigidity during HS. However, adipose tissue stearic acid and SFA content were not affected by HS. Serum fatty acid composition is a balance of fatty acids coming from the diet, adipose tissue lipolysis, and tissue uptake. Circulating FFA composition to some extent reflects the fatty acid composition in adipose tissue (Yew Tan et al., 2015). Thus, lower serum stearic acid and SFA may also reflect reduced lipolysis from adipose tissue. Overall, fatty acid profile of adipose tissue was not affected by treatment. This may reflect the in vivo complexity of HS adaptation that causes no distinct changes in tissue fatty acid composition. Overall, these results show a clear difference between the in vitro and in vivo settings in the separation of metabolite profile by metabolomics approach.

In summary, the data provided represent a comprehensive overview of the changes in metabolites and individual fatty acids in adipocytes and mesenteric adipose tissue of pigs under HS. We demonstrate that HS induces distinct metabolite profiles. This may have implication for the explanation of the regulation of lipogenesis, fatty acid oxidation, and membrane fluidity in adipose tissue during HS. However, additional work is needed to further elucidate the role that these metabolites and metabolic pathways play in HS adaptation, and whether they could be targeted for optimization of the adaptive response to HS in pigs.

## SUPPLEMENTARY DATA

Supplementary data are available at *Journal of Animal Science* online.

## LITERATURE CITED

Ardilouze, J. L., B. A. Fielding, J. M. Currie, K. N. Frayn, and F. Karpe. 2004. Nitric oxide and beta-adrenergic stimulation are major regulators of preprandial and postprandial subcutaneous adipose tissue blood flow in humans. Circulation 109:47–52. doi:10.1161/01.CIR.0000105681.70455.73

Chang, H. C., I. Seidman, G. Teebor, and M. D. Lane. 1967. Liver acetyl CoA carboxylase and fatty acid synthetase:

relative activities in the normal state and in hereditary obesity. Biochem. Biophys. Res. Commun. 28:682–686.

Christon, R. 1988. The effect of tropical ambient temperature on growth and metabolism in pigs. J. Anim. Sci. 66:3112–3123.

Cruzen, S. M., R. L. Boddicker, K. L. Graves, T. P. Johnson, E. K. Arkfeld, L. H. Baumgard, J. W. Ross, T. J. Safranski, M. C. Lucy, and S. M. Lonergan. 2015. Carcass composition of market weight pigs subjected to heat stress in utero and during finishing. J. Anim. Sci. 93:2587–2596. doi:10.2527/jas.2014-8347

Dymond, M. K. 2015. Mammalian phospholipid homeostasis: homeoviscous adaptation deconstructed by lipidomic data driven modelling. Chem. Phys. Lipids 191:136–146. doi:10.1016/j.chemphyslip.2015.09.003

Enoch, H. G., A. Catalá, and P. Strittmatter. 1976. Mechanism of rat liver microsomal stearyl-CoA desaturase. Studies of the substrate specificity, enzyme-substrate interactions, and the function of lipid. J. Biol. Chem. 251:5095–5103.

Ernst, R., C. S. Ejsing, and B. Antonny. 2016. Homeoviscous adaptation and the regulation of membrane lipids. J. Mol. Biol. 428:4776–4791. doi:10.1016/j.jmb.2016.08.013

Escribá, P. V., J. M. González-Ros, F. M. Goñi, P. K. Kinnunen, L. Vigh, L. Sánchez-Magraner, A. M. Fernández, X. Busquets, I. Horváth, and G. Barceló-Coblijn. 2008. Membranes: a meeting point for lipids, proteins and therapies. J. Cell. Mol. Med. 12:829–875. doi:10.1111/j.1582-4934.2008.00281.x

Feder, M. E., and G. E. Hofmann. 1999. Heat-shock proteins, molecular chaperones, and the stress response: evolutionary and ecological physiology. Annu. Rev. Physiol. 61:243–282. doi:10.1146/annurev.physiol.61.1.243

Folch, J., M. Lees, and G. H. Sloane Stanley. 1957. A simple method for the isolation and purification of total lipides from animal tissues. J. Biol. Chem. 226:497–509.

Geraert, P. A., J. C. Padilha, and S. Guillaumin. 1996. Metabolic and endocrine changes induced by chronic heat exposure in broiler chickens: growth performance, body composition and energy retention. Br. J. Nutr. 75:195–204.

Heath, M. E. 1983. The effects of rearing-temperature on body composition in young pigs. Comp. Biochem. Physiol. A. Comp. Physiol. 76:363–366.

Johnson, J. S., M. V. Sanz Fernandez, N. A. Gutierrez, J. F. Patience, J. W. Ross, N. K. Gabler, M. C. Lucy, T. J. Safranski, R. P. Rhoads, and L. H. Baumgard. 2015. Effects of in utero heat stress on postnatal body composition in pigs: I. Growing phase. J. Anim. Sci. 93:71–81. doi:10.2527/jas.2014–8354

Katsumata, M., H. Yano, N. Ishida, and A. Miyazaki. 1990. Influence of a high ambient temperature and administration of clenbuterol on body composition in rats. J. Nutr. Sci. Vitaminol. (Tokyo). 36:569–578.

Kellner, T. A., L. H. Baumgard, K. J. Prusa, N. K. Gabler, and J. F. Patience. 2016. Does heat stress alter the pig's response to dietary fat? J. Anim. Sci. 94:4688–4703. doi:10.2527/jas.2016-0756

Krishnan, N., M. B. Dickman, and D. F. Becker. 2008. Proline modulates the intracellular redox environment and protects mammalian cells against oxidative stress. Free Radic. Biol. Med. 44:671–681. doi:10.1016/j.freeradbiomed.2007.10.054

Kubow, K. E., R. Vukmirovic, L. Zhe, E. Klotzsch, M. L. Smith, D. Gourdon, S. Luna, and V. Vogel. 2015. Mechanical forces regulate the interactions of fibronectin and collagen I in extracellular matrix. Nat. Commun. 6:8026. doi:10.1038/ncomms9026

Leach, M. D., and L. E. Cowen. 2014. Membrane fluidity and temperature sensing are coupled via circuitry comprised of Ole1, Rsp5, and Hsf1 in *Candida albicans*. Eukaryot. Cell 13:1077–1084. doi:10.1128/EC.00138-14

van Meer, G., D. R. Voelker, and G. W. Feigenson. 2008. Membrane lipids: where they are and how they behave. Nat. Rev. Mol. Cell Biol. 9:112–124. doi:10.1038/nrm2330

NRC. 2012. Nutrient requirements of swine. National Academy Press, Washington, DC.

Qu, H., S. S. Donkin, and K. M. Ajuwon. 2015. Heat stress enhances adipogenic differentiation of subcutaneous fat depot-derived porcine stromovascular cells. J. Anim. Sci. 93:3832–3842. doi:10.2527/jas.2015-9074

Qu, H., H. Yan, H. Lu, S. S. Donkin, and K. M. Ajuwon. 2016. Heat stress in pigs is accompanied by adipose tissue-specific responses that favor increased triglyceride storage. J. Anim. Sci. 94:1884–1896. doi:10.2527/jas.2015-0084

Ramsay, T. G. 2005. Porcine preadipocyte proliferation and differentiation: a role for leptin? J. Anim. Sci. 83:2066–2074. doi:10.2527/2005.8392066x

Sanz-Fernandez, M. V., S. K. Stoakes, M. Abuajamieh, J. T. Seibert, J. S. Johnson, E. A. Horst, R. P. Rhoads, and L. H. Baumgard. 2015. Heat stress increases insulin sensitivity in pigs. Physiol. Rep. 3:e12478. doi:10.14814/phy2.12478

Schmidt, P., and E. M. Widdowson. 1967. The effect of a low-protein diet and a cold environment on calorie intake and body composition in the rat. Br. J. Nutr. 21:457–465.

Smith, S. 1994. The animal fatty acid synthase: one gene, one polypeptide, seven enzymes. Faseb J. 8:1248–1259.

Stuehr, D. J. 2004. Enzymes of the L-arginine to nitric oxide pathway. J. Nutr. 134(10 Suppl):2748S–2751S; discussion 2765S–2767S. doi:10.1093/jn/134.10.2748S

Vigh, L., B. Maresca, and J. L. Harwood. 1998. Does the membrane's physical state control the expression of heat shock and other genes? Trends Biochem. Sci. 23:369–374.

Wu, H., A. D. Southam, A. Hines, and M. R. Viant. 2008. High-throughput tissue extraction protocol for NMR- and MS-based metabolomics. Anal. Biochem. 372:204–212. doi:10.1016/j.ab.2007.10.002

Yew Tan, C., S. Virtue, S. Murfitt, L. D. Roberts, L. D. Robert, Y. H. Phua, M. Dale, J. L. Griffin, F. Tinahones, P. E. Scherer, et al. 2015. Adipose tissue fatty acid chain length and mono-unsaturation increases with obesity and insulin resistance. Sci. Rep. 5:18366. doi:10.1038/srep18366